Pressure-induced structural phase transitions in UIr

H. Kotegawa,[1,*] S. Araki,[1] T. Akazawa,[2] A. Hori,[1] Y. Irie,[1] S. Fukushima,[1] H. Hidaka,[1] T. C. Kobayashi,[1] K. Takeda,[3] Y. Ohishi,[4] K. Murata,[5] E. Yamamoto,[6] S. Ikeda,[6] Y. Haga,[6] R. Settai,[7] and Y. Ōnuki[7]

[1]*Graduate School of Natural Science and Technology, Okayama University, Okayama 700-8530, Japan*

[2]*Faculty of Maritime Sciences, Kobe University, Higashi-Nada, Kobe 658-0072, Japan*

[3]*Department of Electrical and Electronic Engineering, Muroran Institute of Technology, Muroran, Hokkaido 050-8585, Japan*

[4]*Japan Synchrotron Radiation Research Institute, Sayo, Hyogo 679-5198, Japan*

[5]*Division of Molecular Materials Science, Graduate School of Science, Osaka City University, Osaka 558-8585, Japan*

[6]*Advance Science Research Center, Japan Atomic Energy Research Institute, Tokai, Ibaraki 319-1195, Japan*

[7]*Graduate School of Science, Osaka University, Toyonaka, Osaka 560-0043, Japan*

(Received 10 May 2011; revised manuscript received 16 July 2011; published 10 August 2011)

Strain and resistivity measurements in UIr showed the occurrence of two structural phase transitions under high pressure, indicating the existence of three phases I–III, with slightly different crystal structures. It is suggested that ferromagnetic phases FM1–FM3 emerge in phases I–III, respectively. The pressure-temperature phase diagram was sensitive to the hydrostaticity of pressure. FM3 and superconductivity are observed in the measurements in which Daphne 7373 is used as a pressure-transmitting medium; however they are both absent in the case where petroleum ether is used as a pressure-transmitting medium. These results indicate a close relationship between ferromagnetism and superconductivity.

DOI: 10.1103/PhysRevB.84.054524 PACS number(s): 74.62.Fj, 62.50.−p, 74.25.Dw, 75.30.Kz

I. INTRODUCTION

Superconductivity in crystals without space-inversion symmetry has been intensively researched to investigate its exotic pairing mechanism. In a noncentrosymmetric crystal, spin-orbit coupling leads to the lifting of spin degeneracy. Since the momentum degeneracy of $\boldsymbol{k}$ and $-\boldsymbol{k}$ remains even in such a situation, this symmetry breaking is believed to induce a mixture of spin-singlet and spin-triplet pairing. Recently, many noncentrosymmetric superconductors have been discovered and their unusual pairing symmetry has been discussed.[1–10] In most cases, this sort of superconductivity appears in materials in a paramagnetic or an antiferromagnetic state. Further, in a crystal without space-inversion symmetry, if the time-reversal symmetry is broken by the finite magnetic field, then the momentum degeneracy is also lifted. When the splitting of $\boldsymbol{k}$ and $-\boldsymbol{k}$ is sufficiently larger than the superconducting gap, superconductivity is unrealized in principle. The superconductivity in noncentrosymmetric UIr appears in a ferromagnetic (FM) state in absence of both time-reversal and space-inversion symmetries.[2,3,11] This feature is in sharp contrast to other FM superconductors such as UGe_2, URhGe, and UCoGe, which all possess the inversion symmetry in their crystals.[12–14]

The crystal structure of UIr, shown in Fig. 1, is of monoclinic PbBi-type (space group $P2_1$) and lacks the mirror plane along any direction.[15] The magnetic property is an itinerant ferromagnet with Ising-like anisotropy.[16] The magnetic easy axis is along the [1 0 $\bar{1}$] direction, and the Curie temperature is $T_{c1} = 46$ K.[17] Three FM phases, denoted as FM1–FM3, are clearly observed from ac-susceptibility measurements under pressure,[11] but no anomaly was observed for FM2 in AC calorimetry measurement.[18] Superconductivity with a transition temperature (T_{sc}) of 0.14 K is observed in a narrow pressure range just below the critical pressure of FM3 at around 2.7–2.8 GPa.[11] The simultaneous observation of superconductivity and non-Fermi liquid behavior of $T^{5/3}$ dependence in the resistivity suggests that the FM critical fluctuation plays an important role in the occurrence of superconductivity.[3] However, the origin of three different FM phases in UIr is an unsolved issue. In addition, the previous ac-susceptibility measurement showed that the volume fraction of the diamagnetic response is roughly 5% of the full Meissner signal.[11] A long coherence length of 1100 Å, which is comparable to the mean free path of 1270 Å, might result in impurity scattering which prevents bulk superconductivity;[3,19] however, it is unclear why the superconducting volume fraction is so small.

In this paper, we conducted resistivity and strain measurements using pressure-transmitting media with better hydrostaticity than that of media used in the previous measurements[3,11] to clearly understand the phase diagram of UIr from the structural aspect. The newly obtained pressure-temperature phase diagram suggests the existence of three structural phases I–III under pressure. The three ferromagnetic phases FM1–FM3 are ascribed to the magnetic ground states for phases I–III, respectively. It is suggested that superconductivity occurs in phase III together with FM3.

II. EXPERIMENTAL PROCEDURE

For measuring the pressure dependences of the resistance and the strain ($\Delta b/b$) at room temperature, we used a piston-cylinder cell and Daphne 7474 as a pressure-transmitting medium.[20] The $\Delta b/b$ is measured by means of the strain gauge method. The applied pressure was estimated from the resistance of a manganin wire. For measuring the temperature dependence of the resistivity (ρ) at several pressures, we used an indenter type of pressure cell[21] and compared the results for two media: petroleum ether and Daphne 7373. The pressure (P) was estimated at low temperatures from the superconducting transition temperature T_{sc} of lead: $P = [T_{sc}(0) - T_{sc}(P)]/0.37$ GPa. The decrease in pressure from room temperature to low temperature is estimated to be approximately 0.2–0.4 GPa in the indenter cell with Daphene

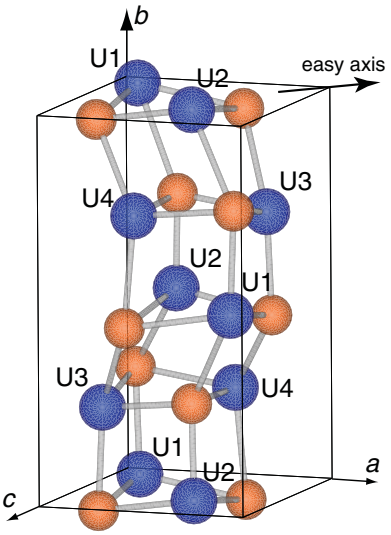

FIG. 1. (Color online) Crystal structure of UIr. The crystal does not possess the inversion center in any direction. The easy axis of the magnetic moment is along the [1 0 $\bar{1}$] direction.

7373. In the case of petroleum ether, which is similar to a mixture of *n* pentane and isopentane, the decrease in pressure is expected to be somewhat larger than that of Daphne 7373.[22] The residual resistivity ratio (RRR) of the sample used in these measurements was 230 when the current flowed along the [1 0] direction. The resistivity was measured using a four-probe method. An x-ray diffraction experiment under high pressure and room temperature was carried out using single-crystalline samples at BL10XU, SPring-8. A diamond anvil cell (DAC) was utilized using a 4:1 mixture of methanol/ethanol as a pressure-transmitting medium. Pressure was estimated by the ruby fluorescence method.

III. PRESSURE-INDUCED STRUCTURAL PHASE TRANSITION

Figure 2 shows the pressure dependences of the strain ($\Delta b/b$) and the resistance along [0 1 0], measured at room temperature. We used Daphne 7474 for these measurements as a pressure-transmitting medium. Daphne 7474 does not solidify in this pressure range, ensuring hydrostaticity.[20] The $\Delta b/b$ shows two distinct drops at ∼2.0 and ∼2.2 GPa on increasing pressure. Both anomalies show hysteresis against pressure, clearly indicating two first-order transitions. The transition at higher pressure is found to affect the resistance. These phases are denoted as I–III from the lower pressure side.

In the previous x-ray powder diffraction measurement conducted under pressure, the broad diffraction pattern due to the damaged fine powder did not ensure a reliable analysis.[11] Therefore, in this study, we performed an x-ray diffraction measurement for a single crystal. The pressure dependences of lattice constants and angle β between the a and c axes are shown in Fig. 3. Each lattice constant decreases and β increases monotonously, as the pressure increases, without an obvious change at around 2 GPa. The structural changes at the phase transitions are expected to be less than the experimental

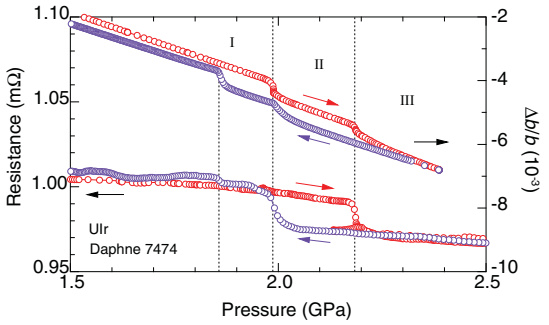

FIG. 2. (Color online) Pressure dependence of resistance along [0 1 0] and that of $\Delta b/b$, at room temperature. First-order transitions with clear hysteresis were observed in both measurements. We define these phases as I–III.

accuracy, because the change along the b axis is less than 0.1%. It was previously suggested that the space-inversion symmetry is still lacking even at phases II and III, because the diffraction pattern does not show a drastic change from $P2_1$ to the neighboring structure with inversion symmetry (e.g., $P2_1/m$).[11] These results indicate that the two structural phase transitions are accompanied by only slight changes in the crystal structure.

Next, we investigated the temperature dependence of ρ along [0 1 0] to determine the boundary between phases II and III down to low temperatures. Figure 4(a) shows the results obtained using petroleum ether as a pressure-transmitting medium. Petroleum ether does not solidify at room temperature in this pressure range.[23] As shown in the inset, the first-order transition with large hysteresis is observed at 2.53 GPa, indicating the transition between phase III and phase II. The transition temperatures T_S^c and T_S^h are defined

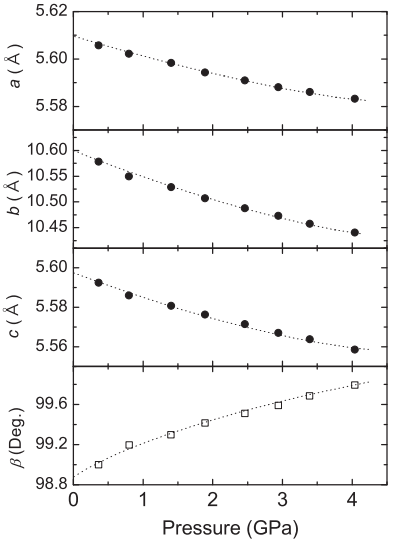

FIG. 3. Pressure dependences of the lattice constants and the angle β between the a and c axes at room temperature. Each lattice constant and β changed without any anomaly at around 2.0–2.2 GPa within the experimental accuracy. The compressibility along the b axis is roughly twice those of other axes.

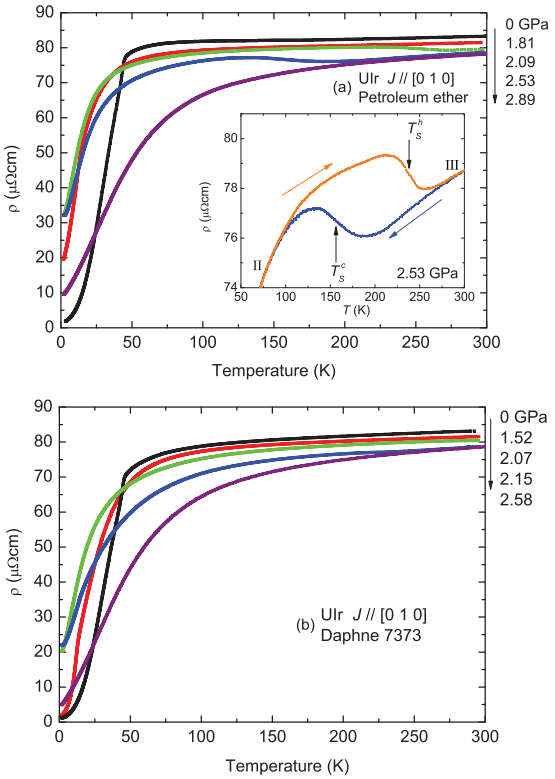

FIG. 4. (Color online) Temperature dependence of ρ along [0 1 0] using (a) petroleum ether and (b) Daphne 7373. The results on cooling are plotted. The inset shows the hysteresis between T_S^c and T_S^h, which denote the midpoints in the jumps on cooling and heating, respectively.

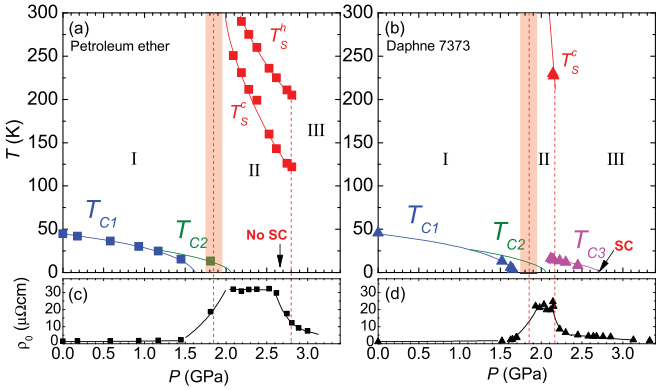

FIG. 5. (Color online) Pressure-temperature phase diagrams and pressure dependences of ρ_0. (a) In the case of the measurement using petroleum ether, the phase transition from III to II occurs with decreasing temperature, and both FM3 and the superconducting phases simultaneously disappear. (b) In the case of the measurement using Daphne 7373, phase III survives even at low temperatures, and the transition to FM3 and the emergence of superconductivity are observed at around 2.7 GPa. The boundary between phases I and II is ∼2.0 GPa at room temperature. The pressure dependence of ρ_0 suggests that the boundary between phases I and II is vertical against pressure.

as the midpoints of the jumps in the cooling and heating plot, respectively. This anomaly is smeared out at 2.89 GPa. The residual resistivity ρ_0 is enhanced in the intermediate pressure region, and it decreases at higher pressures.[24] Figure 4(b) shows the results obtained using Daphne 7373 as the pressure-transmitting medium. It is known that Daphne 7373 solidifies above 2.2 GPa at room temperature.[25] At 2.15 GPa, a small anomaly corresponding to the first-order transition at ∼230 K is observed. However, it vanishes at 2.58 GPa, suggesting that phase III does not transform to phase II even at low temperatures.

From these measurements, the pressure-temperature phase diagrams in the cases of petroleum ether and Daphne 7373 are summarized in Figs. 5(a) and 5(b). The pressure dependences of ρ_0 for these media are shown in Figs. 5(c) and 5(d). In the case of petroleum ether, the structural phase transition from III to II and the enhancement of ρ_0 are observed in nearly the same pressure range. This pressure range is wider than that in the case of Daphne 7373. In both cases, the application of pressure enhances ρ_0 above ∼1.7 GPa. On the other hand, the critical pressure, where ρ_0 decreases, strongly depends on the pressure-transmitting medium; ∼2.8 GPa for petroleum ether and ∼2.2 GPa for Daphne 7373. In both cases, the structural transition and the enhancement of ρ_0 disappear simultaneously, which implies that the enhanced ρ_0 is an indicator of phase II. The changes in the crystal structure may induce a topological change in the Fermi surface, resulting in the anisotropic enhancement of ρ_0 in phase II. The phase boundary between I and II is around 2.0 GPa at room temperature. The pressure dependence of ρ_0 indicates that the phase boundary between I and II is almost vertical against pressure, as shown in Figs. 5(a) and 5(b). The freezing pressures at room temperature are 2.2 GPa for Daphne 7373[20] and 6 GPa for petroleum ether.[23] The freezing of Daphne 7373 seems to prevent the transformation from phase III to phase II upon cooling, which probably requires an increase in volume. It may be considered that, in general, the hardness of the frozen medium prevents the structural transition that occurs with the increase in volume.

IV. RELATIONSHIP BETWEEN FM3 AND SUPERCONDUCTIVITY

Figure 6 shows the temperature dependence of ρ for petroleum ether and Daphne 7373 at 2.2–2.3 GPa. In the case of Daphne 7373, a kink is observed at $T_{C3} = 13$ K, corresponding to the transition into FM3. In the case of petroleum ether, ρ_0 is still high, with no anomaly at T_{C3}. As shown in Fig. 5(a), the anomaly at T_{C3} does not appear at any pressure in the case of petroleum ether. The difference in the phase diagrams suggests that FM3 is realized in phase III. It should be noted that when ρ_0 is high, the anomaly at T_{C2} is observed irrespective of media, which is an indicator of phase II. It is deduced from the successive phase transitions that three ferromagnetic phases FM1–FM3 appear in phases I–III, respectively.

Figure 7 shows the temperature dependence of ρ below 0.4 K for the two media. In the case of petroleum ether, high ρ_0 indicates the existence of phase II, and there is no sign of superconductivity at 2.62–2.89 GPa. On the other hand, in the case of Daphne 7373, superconductivity was

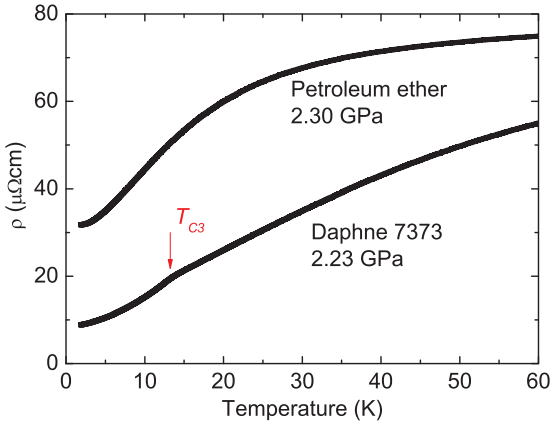

FIG. 6. (Color online) Temperature dependence of ρ for different media at nearly the same pressure of 2.2–2.3 GPa. In the case of Daphne 7373, ρ_0 is low and a kink is observed at T_{C3}; however, the ρ for petroleum ether shows no anomaly.

observed in this study as well as in previous studies.[2,3,11] The absence of both superconductivity and FM3 in the case of petroleum ether suggests that the superconductivity occurs in phase III, that is, intrinsically in the vicinity of the critical point of FM3.

We determined the magnitude of the diamagnetic response in the present sample in the case of Daphne 7373. Figure 8 shows the temperature dependence of ac susceptibility. A clear diamagnetic signal is observed below T_{sc} and is most remarkable at 2.72 GPa, but the volume fraction is estimated to be ∼19%. As shown in Fig. 5(d), the continuous reduction of ρ_0 at around 2.7 GPa may suggest that phase III at low temperature is not a single phase yet. A small fraction of phase II may be responsible for preventing the bulk superconductivity.

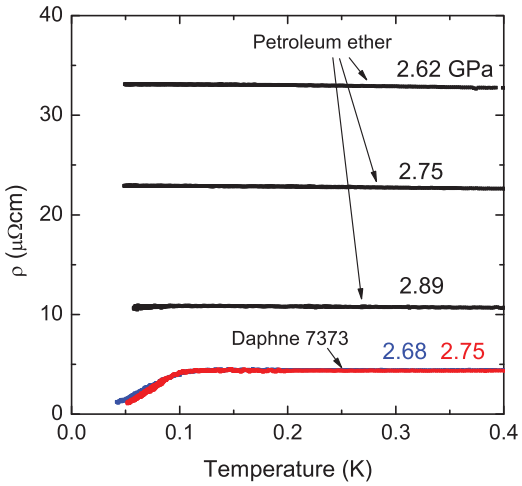

FIG. 7. (Color online) Temperature dependence of ρ below 0.4 K for $J \parallel [0\ 1\ 0]$ using petroleum ether and Daphne 7373. In the case of petroleum ether, ρ_0 is high and superconductivity is absent. In the case of Daphne 7373, ρ_0 decreases in this pressure range and superconductivity appears. Zero resistance is clearly observed in the case of $J \parallel [1\ 0\ \bar{1}]$.[2,3,11]

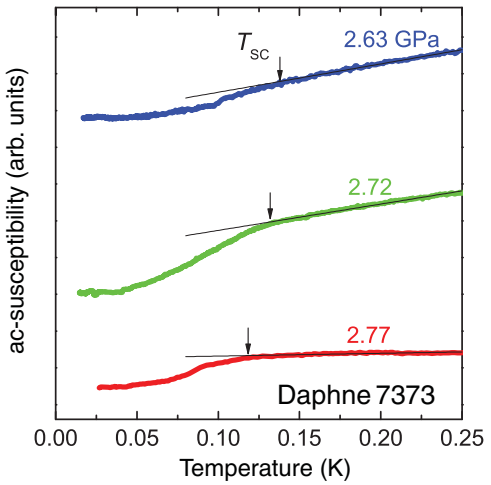

FIG. 8. (Color online) Temperature dependence of ac susceptibility. The diamagnetic signal can be observed clearly, but the volume fraction is ∼19%.

V. CONCLUSION

Resistivity and strain measurements of UIr indicate that hysteresis appears against pressure for $J \parallel [0\ 1\ 0]$, providing clear evidence that three structural phases exist in UIr. The detailed analysis of the x-ray diffraction measurements was difficult at present, owing to the experimental accuracy. The transition from phase III to phase II upon cooling depends on the pressure-transmitting medium, probably whether the medium is solid or liquid. In the case of Daphne 7373, phase III survives down to low temperature, and FM3 and superconductivity are observed. On the other hand, in the case of petroleum ether, phase III transforms to phase II at low temperatures. Phase II possesses a high-ρ_0 state, and superconductivity does not appear in this situation. The different phase diagrams of the two media suggest that superconductivity intrinsically appears in the vicinity of FM3. However, the superconducting volume fraction was ∼19% from the ac-susceptibility measurement. Even for Daphne 7373, ρ_0 in the pressure region of the superconductivity is ∼4.4 $\mu\,\Omega$ cm, which is still higher than ∼1.5 $\mu\,\Omega$ cm at ambient pressure, and it gradually decreases even above ∼2.7 GPa. This indicates that a small fraction of phase II remains at low temperature, even in the case of Daphne 7373. For achieving bulk superconductivity in UIr, it is necessary to obtain phase III as a single phase at ∼2.7 GPa.

ACKNOWLEDGMENTS

This work has been partially supported by Grants-in-Aid for Scientific Research [No. 20740197, No. 20340090, and No. 20102008 (Innovative Area “Heavy Electrons”)] from the Ministry of Education, Culture, Sports, Science, and Technology (MEXT) of Japan. The synchrotron radiation experiments were performed at BL10XU in SPring-8 with the approval of the Japan Synchrotron Radiation Research Institute (Proposal No. 2007B1549).

*Present address: Department of Physics, Kobe University, Kobe 657-8501, Japan

[1]E. Bauer, G. Hilscher, H. Michor, Ch. Paul, E. W. Scheidt, A. Gribanov, Yu. Seropegin, H. Noël, M. Sigrist, and P. Rogl, Phys. Rev. Lett. **92**, 027003 (2004).

[2]T. Akazawa, H. Hidaka, T. Fujiwara, T. C. Kobayashi, E. Yamamoto, Y. Haga, R. Settai, and Y. Ōnuki, J. Phys. Condens. Matter **16**, L29 (2004).

[3]T. Akazawa, H. Hidaka, H. Kotegawa, T. Fujiwara, T. C. Kobayashi, E. Yamamoto, Y. Haga, R. Settai, and Y. Ōnuki, J. Phys. Soc. Jpn. **73**, 3129 (2004).

[4]N. Kimura, K. Ito, K. Saitoh, Y. Umeda, H. Aoki, and T. Terashima, Phys. Rev. Lett. **95**, 247004 (2005).

[5]I. Sugitani, Y. Okuda, H. Shishido, T. Yamada, A. Thamizhavel, E. Yamamoto, T. D. Matsuda, Y. Haga, T. Takeuchi, R. Settai, and Y. Ōnuki, J. Phys. Soc. Jpn. **75**, 043703 (2006).

[6]H. Q. Yuan, D. F. Agterberg, N. Hayashi, P. Badica, D. Vandervelde, K. Togano, M. Sigrist, and M. B. Salamon, Phys. Rev. Lett. **97**, 017006 (2006).

[7]M. Nishiyama, Y. Inada, and G.-Q. Zheng, Phys. Rev. Lett. **98**, 047002 (2007).

[8]A. D. Hillier, J. Quintanilla, and R. Cywinski, Phys. Rev. Lett. **102**, 117007 (2009).

[9]E. Bauer, G. Rogl, X.-Q. Chen, R. T. Khan, H. Michor, G. Hilscher, E. Royanian, K. Kumagai, D. Z. Li, Y. Y. Li, R. Podloucky, and P. Rogl, Phys. Rev. B **82**, 064511 (2010).

[10]A. B. Karki, Y. M. Xiong, I. Vekhter, D. Browne, P. W. Adams, D. P. Young, K. R. Thomas, J. Y. Chan, H. Kim, and R. Prozorov, Phys. Rev. B **82**, 064512 (2010).

[11]T. C. Kobayashi, A. Hori, S. Fukushima, H. Hidaka, H. Kotegawa, T. Akazawa, K. Takeda, Y. Ohishi, and E. Yamamoto, J. Phys. Soc. Jpn. **76**, 051007 (2007).

[12]S. S. Saxena, P. Agarwal, K. Ahilan, F. M. Grosche, R. K. W. Haselwimmer, M. J. Steiner, E. Pugh, I. R. Walker, S. R. Julian, P. Monthoux, G. G. Lonzarich, A. Huxley, I. Sheikin, D. Braithwaite, and J. Flouquet, Nature (London) **406**, 587 (2000).

[13]D. Aoki, A. Huxley, E. Ressouche, D. Braithwaite, J. Flouquet, J. P. Brison, E. Lhotel, and C. Paulsen, Nature (London) **413**, 613 (2001).

[14]N. T. Huy, A. Gasparini, D. E. de Nijs, Y. Huang, J. C. P. Klaasse, T. Gortenmulder, A. de Visser, A. Hamann, T. Görlach, and H. v. Löhneysen, Phys. Rev. Lett. **99**, 067006 (2007).

[15]A. Dommann and F. Hullinger, Solid State Commun. **65**, 1093 (1988).

[16]A. Galatanu, Y. Haga, E. Yamamoto, T. D. Matsuda, S. Ikeda, and Y. Ōnuki, J. Phys. Soc. Jpn. **73**, 766 (2004).

[17]E. Yamamoto, Y. Haga, A. Nakamura, Y. Tokiwa, D. Aoki, R. Settai, and Y. Ōnuki, J. Phys. Soc. Jpn. **70**, 37 (2001).

[18]N. Tateiwa, Y. Haga, T. D. Matsuda, E. Yamamoto, S. Ikeda, T. Takeuchi, R. Settai, and Y. Ōnuki, J. Phys. Soc. Jpn. **76**, 140 (2007).

[19]E. Yamamoto, Y. Haga, H. Shishido, H. Nakawaki, Y. Inada, R. Settai, and Y. Ōnuki, Physica B **312–313**, 302 (2002).

[20]K. Murata, K. Yokogawa, H. Yoshino, S. Klotz, P. Munsch, A. Irizawa, M. Nishiyama, K. Iizuka, T. Nanba, T. Okada, Y. Shiraga, and S. Aoyama, Rev. Sci. Instrum. **79**, 085101 (2008).

[21]T. C. Kobayashi, H. Hidaka, H. Kotegawa, K. Fujiwara, and M. I. Eremets, Rev. Sci. Instrum. **78**, 023909 (2007).

[22]H. Fukazawa, K. Hirayama, T. Yamazaki, Y. Kohori, and T. Matsumoto, J. Phys. Soc. Jpn. **76**, 125001 (2007).

[23]M. I. Eremets, *High Pressure Experimental Methods* (Oxford University Press, UK, 1996).

[24]A. Hori, H. Hidaka, H. Kotegawa, T. C. Kobayashi, T. Akazawa, S. Ikeda, E. Yamamoto, Y. Haga, R. Settai, and Y. Ōnuki, J. Phys. Soc. Jpn. **75S**, 82 (2006).

[25]K. Yokogawa, K. Murata, H. Yoshino, and S. Aoyama, Jpn. J. Appl. Phys. **46**, 3636 (2007).